NUMERICAL SIMULATION OF TSUNAMI BORE PRESSURE ON CYLINDRICAL STRUCTURE

Indradi WIJATMIKO[1] and Keisuke MURAKAMI[2]

[1]Member of JSCE, M. Eng., Graduate Student, Interdisciplinary Graduate School of Agriculture and Engineering, University of Miyazaki (1-1 Gakuen Kibanadai Nishi, Miyazaki, 889-2192, Japan)
[2]Member of JSCE, Dr. of Eng., Dept. of Civil and Environmental Engineering, University of Miyazaki (1-1 Gakuen Kibanadai Nishi, Miyazaki, 889-2192, Japan)

津波被害を最小化するためには沿岸構造物の津波に対する安定性を確保することは肝要であり，様々な津波流体力の評価方法が開発されている．本研究では波と構造物の相互干渉解析手法の一つとして開発された数値波動水路（CADMAS-SURF/3D）の段波津波に対する流体力評価や遡上現象評価の適用性を検討した．その結果，数値計算結果は実験結果と良い一致を示すことを確認した．本手法は任意断面形状の構造物に対して適用可能で，円筒構造物に作用する波圧特性について検討した結果，構造物脚部には鉛直壁面に作用する波圧とほぼ同等の波圧が作用する場合があることを示した．

Key Words: *Tsunami, Bore, VOF method, Tsunami force, Tsunami pressure, Cylindrical Structure*

1. INTRODUCTION

Various mitigation strategies have been developed to reduce catastrophic damages during tsunami disasters, e.g. the effective early warning, inundation maps, evacuation plans and increasing tsunami awareness on society. In addition to those countermeasures, it is also important to secure and improve a structural resistance of coastal facilities against tsunami attacks. Failure of these buildings may cause great financial losses, extent the recovery constructions for much longer period and also cause secondary disasters. Therefore the physical understanding of interactions between tsunami wave and structure is imperative.

Tsunami which creates enormous forces usually amplifies in the shallow water area and transfer into bore type when it breaks[1)]. Moreover, the hydrodynamic pressure of bore type tsunamis sometimes becomes larger than the one of gravity waves, and it may cause impulsive force on structures[2)]. Many authors have been investigating the impact of bore wave on the vertical wall structures through experiments and numerical simulations[3-4)]. However only several of them put their interest on the tsunami wave interactions against three-dimensional cylindrical structures as it reassembles many coastal structures, such as columns, pillars, tank storage or tsunami evacuation building's shape.

In order to understand the interactions between tsunami waves and three-dimensional structures, a numerical simulation shows great performance since it gives principal physical quantities, such as a pressure, velocity and free surface elevation, at any points.

Nowadays, three-dimensional numerical simulation has been vastly developed[5-8)]. Among those simulations, the method based on volume of fluid (VOF; CADMAS-SURF[5)]) is considered one of the promising numerical techniques to simulate three-dimensional interactions between tsunami waves and structures.

Therefore this study investigates the applicability of this numerical method to the estimation of wave pressure and wave forces on cylindrical structures above the dike exposed to bore type tsunami. Few researches have been conducted on evaluating the applicability of this numerical model for bore inundation on to a dry dike and its flow around a structure with arbitrary cross section. Some characters of tsunami pressures, including the vertical and horizontal distribution on cylindrical structures are also discussed.

2. EXPERIMENTAL AND NUMERICAL SETUP

(1) Experimental facilities and procedures

Experiments were performed with using an open

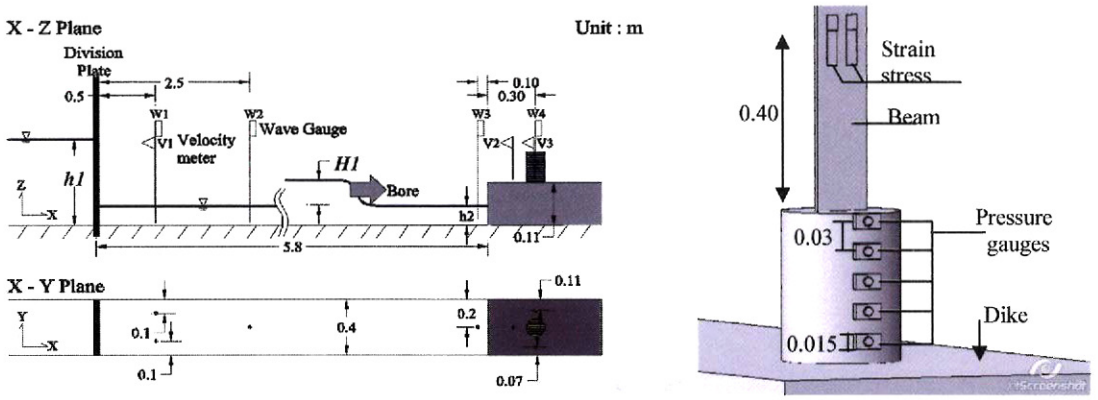

Fig. 1 Experimental setup (unit in meter)

channel of 12m long, 0.4m wide and 0.4m deep as shown in **Fig. 1**. A bore with various different heights (*H1*) was generated by lifting division plate instantaneously which initially separates the downstream quiescent water from the upstream deeper water. The downstream water depth (*h2*) was set in 0.045m. While the water level on upstream side of the division plate (*h1*) was changed in the range from 0.15-0.30m in order to obtain various bore heights.

The model scale was assumed 1/30 in this study. A dike with 0.11m in height was installed on the downstream side 5.8m distance from the division plate. At 0.3m from the dike's corner, a cylindrical structure with different diameter, e.g. 0.04m, 0.08m and 0.11m, was set on the dike. The height of the cylinders was 0.15m. The cylinder was attached to the metal beam to measure the horizontal wave force on it.

Three wave gauges (W1, W2, W3) and one velocity meter (V1) were placed on the propagation area. While in the inundation area, one wave gauge (W4) and one velocity meter (V3) were placed beside the cylindrical structure. One velocity meter (V2) was placed 0.05m in front of cylinder to collect velocity data.

To obtain force data, four stress-strain gauges were attached to the beam as shown in **Fig.1**. A moment equilibrium equation in two points was used to estimate wave force from these gauges. Five pressure gauges were attached to the front face of the cylinder with 0.015m distance between two gauges.

In these experiments, there were 12 cases performed with different configurations; three different diameter sizes had four cases of impoundment height, e.g. *h1*=0.15m, *h1*=0.20m, *h1*=0.25m and *h1*=0.30m.

(2) Numerical simulation configurations

Tsunami bore propagation was simulated through VOF model by CADMAS SURF in similar configurations as experimental setup. The numerical flume size was 8.44m in *X*-axis, 0.4m in *Y* and *Z*-axis, in where the input boundary was set at the location of W1 in **Fig.1**. Therefore the total number of grids was 5.401.600, with grid size of 0.01m in *X*-axis, 0.01m in *Y*-axis and 0.005m in *Z*-axis.

Simulation of bore wave propagation in CADMAS-SURF requires time history of wave surface elevation and wave velocity on the input boundary. In this study, following analytical formula purposed by Fukui et., at[2] was employed to estimate the fluid velocity from water surface elevation on input boundary, because the water surface elevation is commonly measured in experiments and fields in comparison with the fluid velocity:

$$U = \frac{C\zeta}{H} = \zeta\sqrt{\frac{gH(H+h)}{2H(H+\eta\zeta)}} \qquad (1)$$

Where U is the mean velocity, g the acceleration of gravity, $H=h+\zeta$ the total depth from the datum (**Fig. 2**), ζ the temporal bore height. η is the velocity coefficient which equal to 1.03, and was taken from the ratio of water level and wave height.

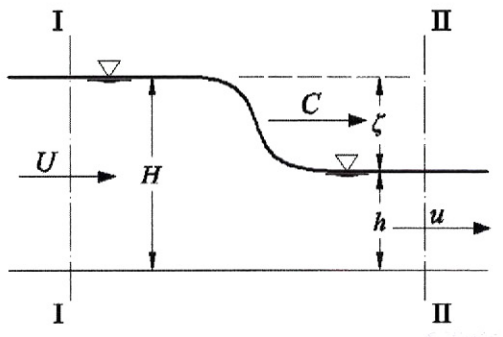

Fig. 2 Bore wave profile

It can be seen in **Fig. 3** that the temporal flow velocities, which are represented by dotted lines,

obtained from **Eq.1** at W1 show good agreement with measured velocities (solid lines) in each impoundment height. In numerical simulation, the time history of both water surface elevation and fluid velocity was applied as matrix data on input boundary at W1.

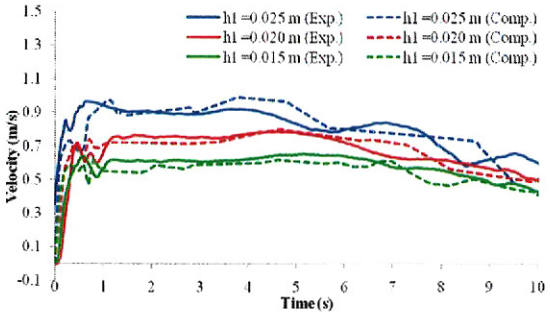

Fig. 3 Velocity profile of experimental and Fukui estimation at station 1(V1)

3. VERIFICATION OF SIMULATION

(1) Water Surface Elevation

Fig. 4 shows the comparison of water surface profiles at propagation area (W2) in case of 0.11m diameter cylindrical structure, where the solid lines mean the measured data in experiment and dot lines mean simulated ones.

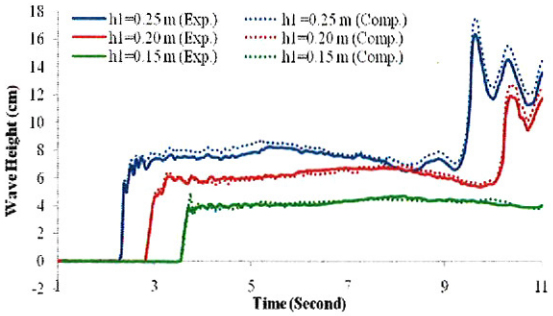

Fig. 4 Water surface elevation at station 2(W2)

In measured data in every impoundment height, bore front face can be identified from the quick raise pattern in the beginning of measurement. And then bore propagated without significant water height changes. At the end, the wave reflection from the dike caused the fluctuations of wave height for case with *h1*=0.2m and *h1*=0.25m. Those dynamic changes in experimental data were simulated fairly good in numerical simulation in every impoundment height.

Fig. 5 shows the water surface profile at 0.05m beside the cylindrical structure (W4) on the dike. In every case, measured bore height quickly increased at the moment of passing the wave gauges. The water depth reached the maximum after a few second, and then it showed decreasing tendency. The water surface profiles obtained from numerical simulation show similar profiles to the experimental results. Though the numerical simulation results were slightly overestimate the maximum water depth that occurs after the bore front passes the wave gauges.

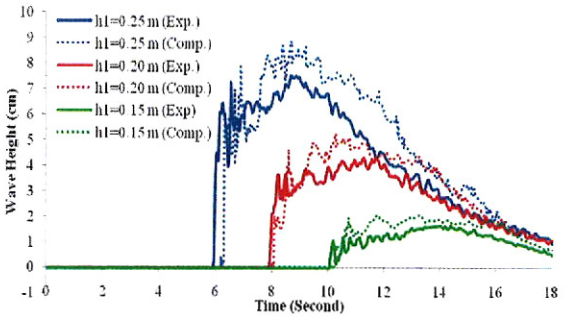

Fig. 5 Water surface elevation at station 4(W4)

(2) Fluid Velocity Profile

Fig. 6 shows fluid velocities in front of 0.11m diameter cylindrical structure on the dike (V2). In all cases, the measured velocities quickly increased in the same manner as the water surface profile in **Fig.4** and **Fig.5**. After taking the maximum value, the velocities rapidly decreased due to the overlap of overtopped flow and reflected one from the cylinder.

As seen in **Fig. 6**, despite the differences at impoundment height, the velocity after the bore front show similar value as the wave completely adjust its flow after hitting the dike wall. Even under these complicated flow conditions, the numerical results show good agreement with experimental ones.

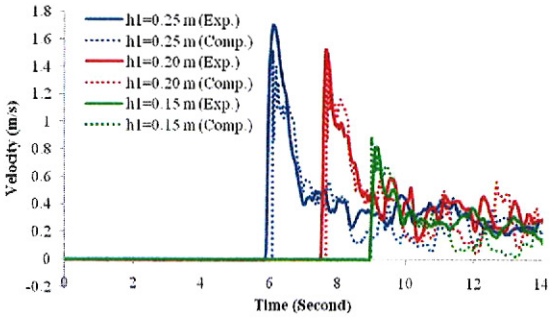

Fig. 6 Fluid velocities at station 2(V2)

Fig. 7 shows the fluid velocities at 0.05m beside of the cylinder (V3). In all impoundment cases, the measured velocities quickly increased and took the maximum values in the same manner with velocities at the station 2, which can be seen in **Fig.6**. And then, velocities started to show the gradual decreasing tendency.

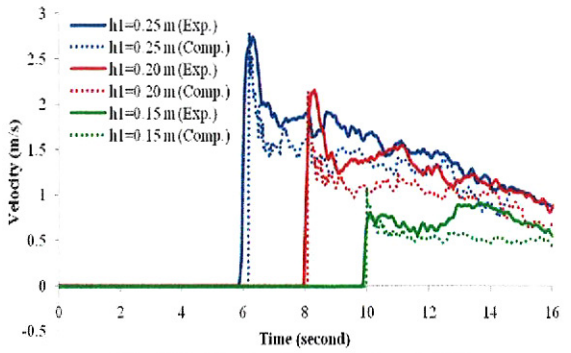

Fig. 7 Fluid velocities at station 3 (V3)

The comparisons between experimental results and numerical ones also show good agreement in each case, though the simulated velocities slightly underestimate the inundated velocities.

(3) Force Profile

Fig. 8 shows the comparison of wave forces acting on the 0.11m diameter of cylindrical structure with 0.25m impoundment height. In experimental results, wave profiles oscillated a little after the bore hit the cylinder. These fluctuations in experiments came from the natural oscillation of measurement system.

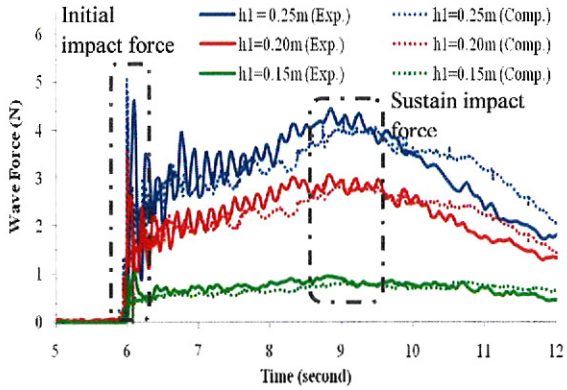

Fig. 8 tsunami force of 250 mm impoundment height acting on the cylindrical structure

As seen in **Fig. 8**, sharply increased initial force can be observed both in experimental data and numerical one when the wave hit the cylindrical structure at the initial contact. While the sustain wave force occurred a couple seconds later when the water surface elevation reached its maximum height on structure's surface. Both of these forces were well observed in the experimental results and numerical ones. These force profiles correspond well with other studies[4,9].

Fig. 9(a) shows the comparison of simulated initial force with measures one, and **Fig. 9(b)** also shows the comparison of sustains force.

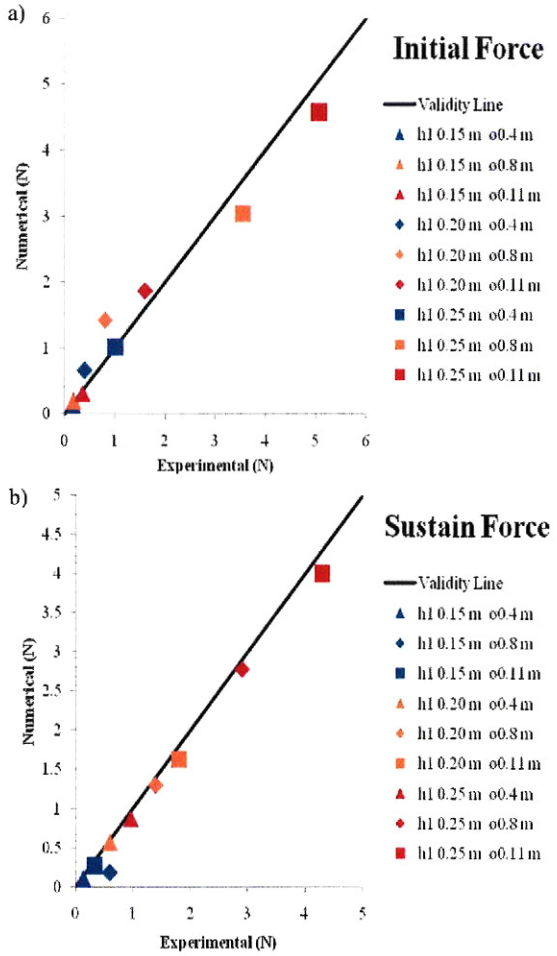

Fig. 9 Validation of wave forces: **(a)** Initial wave forces, and **(b)** Sustain wave forces validation.

Good agreement can be seen both in initial force and sustain one in the wide range of bore height. In the agreement on initial force, a correlation is slightly lower than that in sustain force, because the peak values of impact force usually depend on the sampling frequency of data in experiment and computational time interval in numerical simulation.

From above investigations, it can be concluded that the numerical simulation based on VOF method expanded into three-dimensional problem provide fairly good results even in the complicated inundation process of bore.

3. PRESSURE CHARACTERISTICS

(1) Pressure Profile

Fig. 10 shows the wave pressure profile at the cylindrical surface of 0.11 m diameter structure in case of $h1$=0.15 m. A1, A2 and A3 are the front face with height of 0.001m, 0.02m and 0.04m from the bottom, respectively. While B1, B2, B3 are the diagonal face with 45 degree from the wave direction at the same height level as front face, and

C1, C2 are the side face with height of 0.001m and 0.02m, respectively.

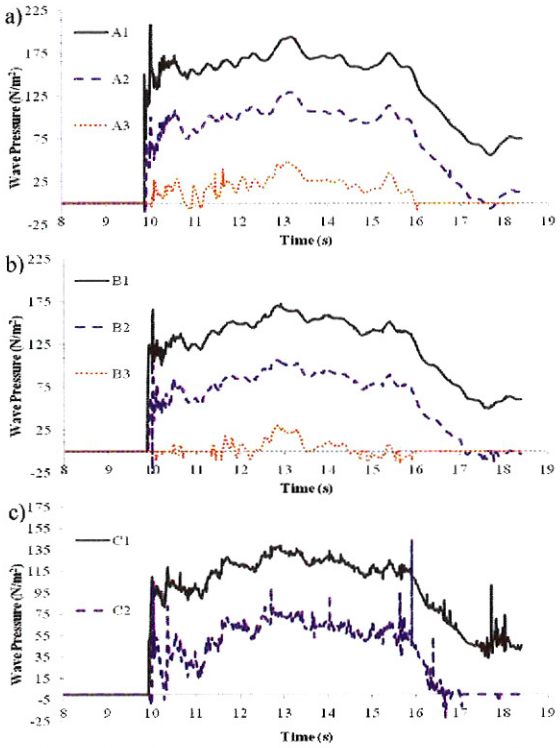

Fig. 10. Wave pressure profile of 0.11m diameter cylindrical structure with impoundment of 0.15m: **(a)** Front face, **(b)** 45 degree from stream direction and **(c)** side face.

It is clear that front face (A1,A2 and A3) received the higher pressure compare to the other faces at the same bore height, and the bottom of the cylinder (A1, B1 and C1) received the highest pressure at each section. The initial impact pressure could be observed well on the points along *A* and *B* section, whereas the sustain pressures are recorded well in all faces. At the height of 0.04m, only side face did not record any pressure, because the measuring point is located above the maximum water surface elevation on this section.

(2) Pressure Distribution

Eq. 2 shows a design pressure distribution on a vertical wall proposed by The Building Technology Research Institute in Japan[10].

$$q_x = \rho g(3h - z) \qquad (2)$$

In this equation, q_x is the desire pressure, ρ the water density, g the acceleration of gravity, h the bore height, and z is the height from the bottom to the desired location. The pressure decreases linearly from $3\rho gh$ at the bottom to zero at $3h$ as shown in **Fig.11**.

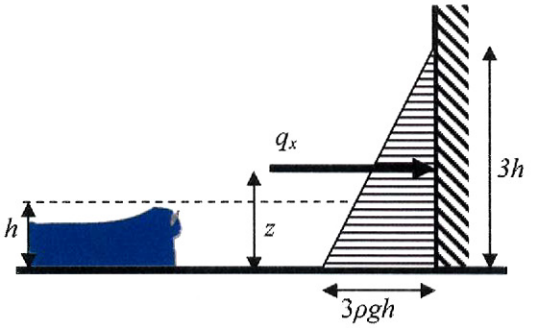

Fig. 11 Designed tsunami wave pressure distribution

Fig. 12 shows the normalized vertical wave pressure distributions on the front face of the cylinder with diameter of 0.11m. The distributions of the wave pressure calculated from **Eq.2** are also plotted in this figure with dashed lines. Normalized wave pressure was obtained from the divided computed or calculated wave pressure by ρgh.

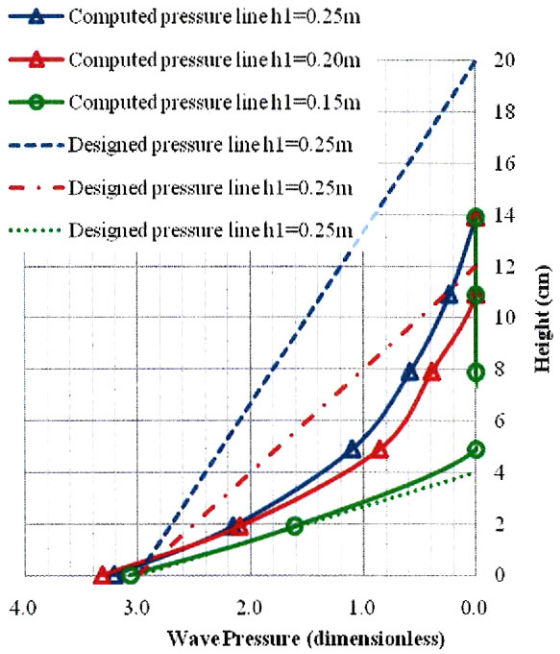

Fig. 12 Vertical wave pressure distribution against cylindrical structure with 0.11m diameter size

Nonlinear pressure distribution on the front face of the cylinder can be observed in each case. At the bottom section, the pressures show the same or even excess value to the designed pressures. On the other hand, the difference of pressure between cylinder and vertical wall increases to upward direction. The bore propagating on the dry bed generates nearly the same wave pressure as a vertical structure at its foot even in the case of cylindrical structure.

This huge pressure at the foot of cylindrical structures may cause serious threats to the stabilities

against the bore tsunami, such as the instability of foundation or the whole structure to failure. Therefore much further study on the force at bottom section needs to be carried out in order to get the better understanding.

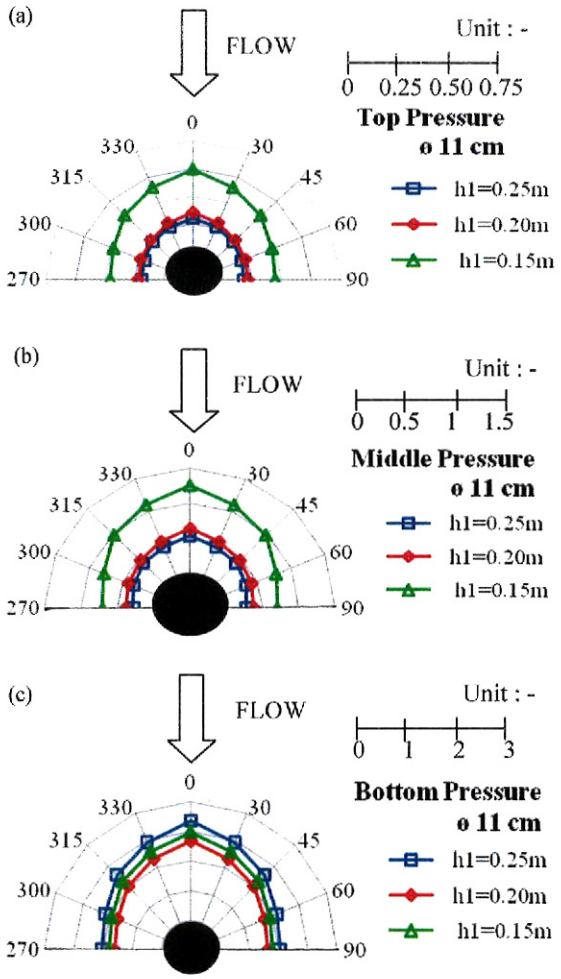

Fig. 13 Horizontal wave pressure distribution on ø 0.11m structure: **(a)** at top section, **(b)** at middle section and **(c)** at bottom section.

The normalized horizontal wave pressure distribution along cylinder faces can be seen in **Fig. 13(a), 13(b)** and **13(c)**. At the bottom section, maximum pressure occured on the front face and it decreased along the cylinder face. The difference of the pressure between front and side face becames larger with the increase of impoundment wave height.

4. CONCLUSIONS

The interactions between a single bore and cylindrical structure are investigate through experimental and numerical study. In the numerical simulation of bore type tsunami, the analytical equation derived by Fukui et., at.[2] can be used to obtained input fluid velocity profile from water surface elevation. The comparison between experimental results and numerical ones showed good agreements in term fluid velocities and water surface elevation on both propagation area and inundation area. Furthermore, good agreements were also confirmed in initial wave forces and sustain ones acting on the cylindrical structure.

In case of bore propagation over the dike, the higher pressure occurred at the bottom section of the vertical cylinder, and the value was similar or exceeding the design pressure on vertical wall. In the horizontal bore pressure distribution, the front face received the highest wave pressure which then the magnitude of wave pressure gradually decreased along the circumferential direction.

REFERENCES

1) Yeh, H. : Tsunami bore runup, *Natural Hazard 4*, pp. 209-220, 1991.
2) Fukui, Y.et. al : Study of tsunami –Investigation of wave velocities in case of bore type tsunami-, *Proc. of Coastal Engineering, JSCE*, Vol. 9, pp.44-49, 1962 (in Japanese).
3) Palermo, D. and Nistor, I. : Understanding tsunami risk to structures : A Canadian perspective, *Science of Tsunami Hazard*, Vol 27, No. 4, pp.1-9, 2008.
4) Haritos, N., Ngo, T., and Mendis, P. : Evaluating tsunami wave force on structure. *International Symposium Disaster Reduction on Coasts Scientific – Sustainable – Holistic - Accesible*. Monash University, Melbourne, Australia 14-16 November 2005.
5) Arikawa, T. and Yamano, T. : Large Scale Simulation on Impulsive Wave Preesures by using CADMAS-SURF/3D, *Annual Journal of Coastal Engineering, JSCE*, Vol.55, pp.26-30, 2008 (in Japanese).
6) Goto, H., Ikari, H. Tonomo, K., Shibata, T, Harada and T., Mizoe, A.: Numerical Analysis on Drifting Behavior of Container on Apron due to Tsunami by Particle Method, *Annual Journal of Coastal Engineering, JSCE*, Vol.56, pp.261-265, 2009 (in Japanese).
7) Tomita, T., Honda, K. and Kakinuma T.: Application of three-dimensional tsunami simulator to estimation of tsunami behavior around structures, *International Conference on Coastal Engineering, ASCE*, pp.1677-1688, 2006.
8) Kawasaki, K., Yamaguchi, S., Hakamada N., Mizutani, N. and Miyajima, S.: Wave Pressure Acting on Drifting Boby after Collision with Bore, *Annual Journal of Coastal Engineering, JSCE*, Vol.53, pp.786-790, 2006 (in Japanese).
9) Lukkunaprasit, P., Ruangrassamee, A., and Thanasisathit, N. : Tsunami loading on buildings with openings, *Science of Tsunami Hazard*, Vol 28, No. 5, pp.303-310, 2009.
10) Okada, T., Sugano, T., Ishikawa, T., Ohgi, T., Takai, S., and Hamabe, C. : Structural design method of building for tsunami resistance (proposed), *Building Technology Research Institute*, the Building Center of Japan, 2004.